International Journal of Engineering Works
https://www.ijew.io/
ISSN-p: 2521-2419
ISSN-e: 2409-2770
Vol. 12, Issue 10, PP. 191-196, October 2025
https:// doi.org/10.5281/zenodo.17360342

Modeling and Analysis of Tumor Growth under Virotherapy, Chemotherapy, and Immune System Dynamics

Siraj Ahmad[1], Zia Ullah Afridi[2], Bibi Shabana[3]
[1,2,3]University of Engineering and Technology Peshawar, Pakistan
sirajkhan5278@gmail.com[1], ziaafridi932@gmail.com[2], shabanasamad.27@gmail.com[3]
Received: 25 September, Revised: 10 October, Accepted: 14 October

***Abstract*—**This study presents a nonlinear mathematical model describing the interaction of uninfected cells, infected cells, viral particles, immune cells (T-cells), and chemotherapy. The analytical results establish that the system preserves biological feasibility, with all state variables remaining positive and bounded over time. Numerical simulations are carried out using biologically motivated parameters, and the results provide insights into the balance between viral replication, immune clearance, and chemotherapy dynamics. The findings highlight the critical role of immune T-cells and chemotherapy factors in shaping the infection outcome and suggest possible directions for improving therapeutic strategies through mathematical analysis.

***Keywords*—**Tumor growth modeling, Virotherapy, Chemotherapy, Immune system dynamics, Nonlinear dynamical systems.

I. Introduction

Cancer remains one of the leading causes of death worldwide, with more than 10 million case reported each year [1]. Researchers developing alleviative treatments for this disease but the work in this area is slow because its show a extremely difficult, multidisciplinary problem requiring wide research and creativity [2]. Oncolytic virotherapy is an developing cancer treatment that uses virus duplication to abolish specifically cancer cells without any harm to normal cells and these viruses have shown efficacy in clinical trial [3,4]. These competent and specific modified viruses which spell tumor cells but not normal cells, that have been made with progresses in the ground of genetic engineering [5].

Oncolytic viruses are investigated to use immunotherapy as a agents for cancer treatment to enhance body immunity. Virotherapy is one of the modern approach that are use the ability of virus to destroy tumor cells to drive an antitumor immune response [6, 15]. This immune response recognize cancer cells as a threat, and trigger that built-in self-destruct mechanism in the cancer cells. While this current approaches have been established to max this immunotherapeutic potential over the accumulation of immunostimulatory cytokines to viral genes or mutual injections of viruses and immune cells [1]. However, there are quiet certain challenges face by oncolytic virotherapy is weather the immune system of the body maybe eliminate the oncolytic virus before they can work Sufficiently, this interference of the immunity potential reduced treatment effectiveness. As a results, the use of oncolytic viruses alone usually doesn't shrink existing tumor cells [3]. Therefore the used of different traditional methods with oncolytic virotherapy like chemotherapy or radiotherapy has gained attention to be promising and killing tumor cells more adequately [2, 7].

In this study, we examine the combined effects of chemotherapy, virotherapy, and immune system activation on tumor dynamics [12, 13]. By integrating these treatment modalities, our goal is to better understand how they influence outcomes when used together [4]. We then apply numerical methods techniques to determine the most accurate approximations of tumor response.

The rest of the paper is organized as follows: Section 2 provides a brief overview of tumor growth models. Section 3 explores the mathematical model of tumor growth Section 4 describes the stability of the proposed model. Finally, Section 5 summarizes findings and discusses possible future research.

II. Mathematical Model Overview

We investigated chemotherapy, logistic growth [6, 8], and introducing some modification in the mathematical model proposed in [8]. In the existing model kim et al.[8], use experimental data to fit parameter values to their suggested model, and then vary treatment strategies to determine the effects of numerous dosage, treatment plans, and targeted viruses have on the short-term (60 days) behavior of the tumor cell populations. The authors conclude that the most important factors in controlling short-term tumor growth are the immune response and the burst size of virous [5, 15]

The progression is exponential for tumor cells in Kim et al. [8], as the information comes from experimental data. Hence, due to ethical care these models do not get the extreme growth of tumor volume as saw in logistic growth. However, in a diversity of models for tumor growth can also be reprsented by Gompertzian [4, 9], and bertalanffy [10, 14] models, these models are popular for modeling in tumor growth because of

mimic real biological processes [7, 11] Built on the related biological suitable, the growth law of tumor cells is considered to be logistic growth [14, 15] giving the connections between tumor cells, drug, virous and the immune cells (T-cells), and the model is express as the following system of six differential equations, where U, I, V, C, and T characterize uninfected tumor cells, infected tumor cells, virotherapy, chemotherapy, and T-cells respectively [8].

$$\frac{dv}{dt} = \alpha + \omega_I - \delta_V V \quad (1)$$

$$\frac{dI}{dt} = \frac{\beta}{N} VU - \gamma_I IT - \delta_I I - \eta_I IC \quad (2)$$

$$\frac{dU}{dt} = rU\left(1 - \frac{U}{k}\right) - \frac{\beta}{N} VU - \gamma_U UT - \eta_U UC \quad (3)$$

$$\frac{dC}{dt} = g - \frac{h_1 C}{h_2 + C} \quad (4)$$

$$\frac{dT}{dt} = \phi_I - \delta_T T \quad (5)$$

Here, we use α is the injection rate of virous, ω_I to represent virous burst size, δ_I represent infected tumor lysis rate, δ_V represent natural death of virous. The injected drug is represent by g and saturation rate of $\frac{h_1 C}{h_2 + C}$, where h_1 is the extreme rate of drug absorption and h_2 is drug concentration drug use rate which is half of h_1. The logistic growth of uninfected tumor volume is represent by r, γ_I, γ_U represent death of infected and uninfected tumor cells due to T-cells respectively, η_I, η_U represent expiry of infected and uninfected tumor cells due to drug respectively, and β characterize the proportion of uninfected cells becoming infected due to virous. The activation of T-cells is represent by ϕ_I while, decay rate is represent by δ_T.

III. ANALYSIS

In this section, we check the positivity, Boundedness, and stability behavior of steady state system:

BONDEDNESS AND POSITIVITY

We now prove the positivity and boundedness of each variable of the model (1-5).

POSITIVITY

For nonnegative initial conditions and parameters, the nonnegative orthant is invariant:

- If $V = 0$, then $\dot{V} = \alpha + \omega_I(I) \geq 0$.
- If $I = 0$, then $\dot{I} = \frac{\beta}{N} VU \geq 0$.
- If $U = 0$, then $\dot{U} = 0$.
- If $C = 0$, then $\dot{C} = g \geq 0$.
- If $T = 0$, then $\dot{T} = \phi_I \geq 0$.

Thus, V, I, U, C, T remain nonnegative for all $t \geq 0$.

BOUNDEDNESS

- $U(t)$ Satisfies $\dot{U} \leq rU(1 - U/k)$, hence $U(t) \leq \max\{U(0), k\}$.
- $T(t)$ Solves a linear ODE, so $E(t) \leq \max\{T(0), \phi_I / \delta_T\}$.
- For $C(t)$, the scalar equation admits an equilibrium $C^* = \frac{g h_2}{h_1 - g}$ (if $h_1 > g$), giving $C(t) \leq \max\{C(0), C^*\}$.
- For (V, I), using $\omega_I(I) \leq cI$ and $U \leq k$, we obtain the comparison system

$$\dot{V} \leq \alpha + cI - \delta_V V, \dot{I} \leq \frac{\beta k}{N} V - \delta_I I$$

If $\delta_V \delta_I > c \frac{\beta k}{N}$, then (V, I) are uniformly bounded.

Hence, all variables remain positive and bounded, and solutions lie in a compact, positively invariant region $\Omega \subset \mathbb{R}^5_+$.

IV. STABILITY ANALYSIS OF THE EQUILIBRIUM POINT

The analysis of the mathematical model (1) since a qualitative insight initiates with finding the system's equilibrium points. To catch the equilibrium points of the system, we recognized:

$$\frac{dV}{dt} = \frac{dU}{dt} = \frac{dI}{dt} = \frac{dC}{dt} = \frac{dT}{dt} = 0.$$

$$0 = \alpha + \omega_I - \delta_V V \quad (6)$$

$$0 = \frac{\beta}{N} VU - \gamma_I IT - \delta_I I - \eta_I IC \quad (7)$$

$$0 = rU\left(1 - \frac{U}{k}\right) - \frac{\beta}{N} VU - \gamma_U UT - \eta_U UC \quad (8)$$

$$0 = g - \frac{h_1 C}{h_2 + C} \quad (9)$$

$$0 = \phi_I - \delta_T T \quad (10)$$

and solving the system (6-10) we get following equilibrium points

$$E = (V^*, U^*, I^*, C^*, T^*, A^*)$$

Where

$$T^* = \frac{\phi_I}{\delta_T} \quad (11)$$

$$C^* = \frac{g h_2}{h_1 - g} \quad (12)$$

$$I^* = \frac{\alpha\beta k}{\delta_V}\left(\frac{\delta_T}{\gamma_I \phi_I} + \frac{1}{\delta_I} - \frac{\gamma_U}{r\gamma_I} - \frac{\gamma_r \phi_I}{\delta_T r \delta_I}\right) + \frac{\beta k (h_1 - g)}{\delta_V \eta_I r g h_2}$$

$$\left(\omega_I + \alpha r - \frac{2\alpha\beta\omega_I}{\delta_V} - \frac{\beta\omega_I^2}{\delta_V} - \frac{\alpha\gamma_U\phi_I}{\delta_T} - \frac{\omega_I\gamma_U\phi_I}{\delta_T} - \frac{\alpha^2\beta}{\delta_V}\right)$$

$$+\frac{\beta\omega_I k}{\delta_V}\left(\frac{1}{\delta_I}+\frac{\delta_T}{\gamma_I\phi_I}-\frac{2\beta}{r\delta_V\gamma_I\phi_I}-\frac{2\beta}{r\delta_V\delta_I}-\frac{\beta\omega_I\delta_T}{r\delta_V\gamma_I\phi_I}\right.$$
$$\left.-\frac{\beta\omega_I}{r\delta_V\delta_I}-\frac{\gamma_U}{\gamma_I r}-\frac{\gamma_U\phi_I}{r\delta_T\delta_I}-\frac{\eta_V}{r\eta_I}\right)-\frac{k\alpha^2\beta^2}{r\delta_V^2}\left(\frac{\delta_T}{\gamma_I\phi_I}+\frac{1}{\delta_I}\right)$$
$$-\frac{\alpha\beta k\eta_V g h_2}{\delta_V r(h_1-g)}\left(\frac{\delta_T}{\gamma_I\phi_I}+\frac{1}{\delta_I}\right)-\frac{\beta\omega_I k\eta_V g h_2}{r\delta_V(h_1-g)}\left(\frac{\delta_T}{\eta_I\phi_I}-\frac{1}{\delta_I}\right)$$
$$-\frac{\alpha\beta k\eta_V}{\delta_V r\eta_I} \quad (13)$$

$$V^*=\frac{\alpha+\omega_I}{\delta_V} \quad (14)$$

$$U^*=k-\frac{k\beta(\alpha+\omega_I)}{r\delta_V}-\frac{k\gamma_U\phi_I}{r\delta_T}-\frac{k\eta_U g h_2}{r(h_1-g)} \quad (15)$$

Jacobian matrix of the model corresponding to the (11-15) fixed point is:

$$\boldsymbol{J_E}=\begin{pmatrix}-\boldsymbol{\delta_v} & \mathbf{0} & \mathbf{0} & \mathbf{0} & \mathbf{0}\\ \boldsymbol{\beta U^*} & \boldsymbol{r-2+H_1} & \mathbf{0} & \boldsymbol{\gamma_U U^*} & \boldsymbol{\eta_U U^*}\\ \boldsymbol{\beta U^*} & \dfrac{\boldsymbol{\beta(\alpha+\omega_I)}}{\boldsymbol{\delta_V}} & \boldsymbol{H_2} & \boldsymbol{-\gamma_I I^*} & \boldsymbol{-\eta_I I^*}\\ \mathbf{0} & \mathbf{0} & \mathbf{0} & \boldsymbol{-\delta_E} & \mathbf{0}\\ \mathbf{0} & \mathbf{0} & \mathbf{0} & \mathbf{0} & \boldsymbol{-\dfrac{h_3^3 h_2 g}{(h_1^2 g-g h_2)^2}}\end{pmatrix} \quad (\mathbf{16})$$

Where

$$\boldsymbol{H_1}=-\tfrac{2\beta(\alpha+\omega_I)}{r\delta_V}-\tfrac{2\gamma_U\phi_I}{r\delta_T}-\tfrac{2\eta_U g h_2}{r(h_1-g)}-\tfrac{\beta(\alpha+\omega_I)}{\delta_V}-\tfrac{\gamma_U\phi_I}{\delta_E}-\tfrac{\eta_U g h_2}{h_1-g}$$

$$\boldsymbol{H_2}=-\frac{\boldsymbol{\gamma_I\phi_I}}{\boldsymbol{\delta_E}}-\boldsymbol{\delta_I}-\frac{\boldsymbol{\eta_I g h_2}}{\boldsymbol{h_1-g}}$$

Eigenvalues of matrix (16) are:

$$\boldsymbol{\lambda_1=-\delta_v,\lambda_2=r-2-\frac{2\beta(\alpha+\omega_I)}{r\delta_V}-\frac{2\gamma_U\phi_I}{r\delta_T}-\frac{2\eta_U g h_2}{r(h_1-g)}}$$
$$\boldsymbol{-\frac{\beta(\alpha+\omega_I)}{\delta_V}-\frac{\gamma_U\phi_I}{\delta_E}-\frac{\eta_U g h_2}{h_1-g}}$$
$$\boldsymbol{\lambda_3=-\frac{\gamma_I\phi_I}{\delta_E}-\delta_I-\frac{\eta_I g h_2}{h_1-g},\lambda_4=-\delta_E,\lambda_5=-\frac{h_1^3 h_2 g}{(h_1^2 g-g h_2)^2}}$$

Since the four eigenvalues show negative real parts and no imaginary components. It follows that fixed point (11-15) are stable, if $r<2+\frac{2\beta(\alpha+\omega_I)}{r\delta_V}+\frac{2\gamma_U\phi_I}{r\delta_T}+\frac{2\eta_U g h_2}{r(h_1-g)}+\frac{\beta(\alpha+\omega_I)}{\delta_V}+\frac{\gamma_U\phi_I}{\delta_E}+\frac{\eta_U g h_2}{h_1-g}$. This proposes that the system has a propensity to approach and continue in this equilibrium state at given conditions, regardless of its initial point.

V. Numerical Solution

To illustrate the analytical results and to gain further insight into the dynamics of system (1-5), we now carry out numerical simulations. The model equations are solved using a standard numerical solver for systems of ordinary differential equations with biologically relevant parameter values. All computations are performed with nonnegative initial conditions, ensuring consistency with the positivity and boundedness properties established in the previous section.

The parameter values used in the simulations are summarized in Table 1. These values are chosen from the literature or selected to be within biologically realistic ranges. Subsequent figures present the time evolution of the model variables under these parameter settings, highlighting the interplay between uninfected cells, infected cells, immune response, and control mechanisms.

Table 1: Model parameters used in numerical simulations.

Parameter	Description	Value	Unit
ω	Virus production rate by I	50	day $^{-1}$
δ_V	Virus clearance rate	0.6	day $^{-1}$
R	Growth rate of uninfected cells	0.31	day $^{-1}$
β	Infection rate constant	0.6	day $^{-1}$
K	Carrying capacity of uninfected cells	3×10^9	Cells
γ_U	Killing of U by T	2×10^{-6}	day $^{-1}$
η_I	Killing of I by C	1×10^{-6}	day $^{-1}$
η_U	Killing of U by C	1×10^{-5}	day $^{-1}$
g	Supply rate of C	1.0	day $^{-1}$
h_1	Saturation constant (consumption)	3.0	day $^{-1}$
h_2	Half-saturation constant	1.0	day $^{-1}$
ϕ_I	Effector source rate	2.0	day $^{-1}$
δ_T	Decay rate of T	0.19	day $^{-1}$
γ_I	Killing of I by T	2×10^{-6}	day $^{-1}$
δ_I	Natural death rate of infected cells	5×10^{-5}	day $^{-1}$
N	Normalization factor	1×10^7	Cells

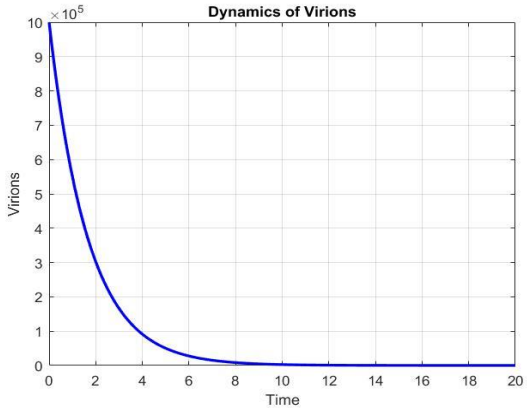

Figure 1: Effect of varying viral clearance rate δ_V on infection outcome.

Figure 1, shows that increasing δ_V significantly reduces viral persistence, lowering infected cell levels and facilitating recovery of uninfected cells. When δ_V is small, viral particles accumulate, driving chronic infection. This suggests that therapeutic strategies targeting viral clearance could be effective in reducing infection burden.

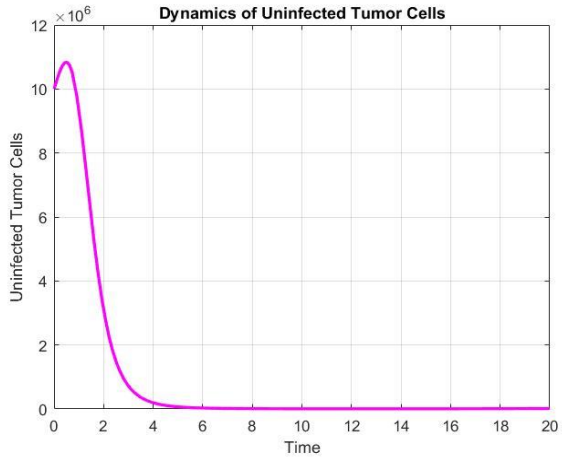

Figure 2: Time evolution of uninfected tumor cells $U(t)$ under baseline parameter values.

Figure 2, shows the dynamics of uninfected tumor cells. At the beginning, U grows steadily, but once viral particles become active, U decreases due to infection and immune-mediated killing. Later, depending on the strength of immune response and viral clearance, U either stabilizes at a reduced level or begins partial recovery.

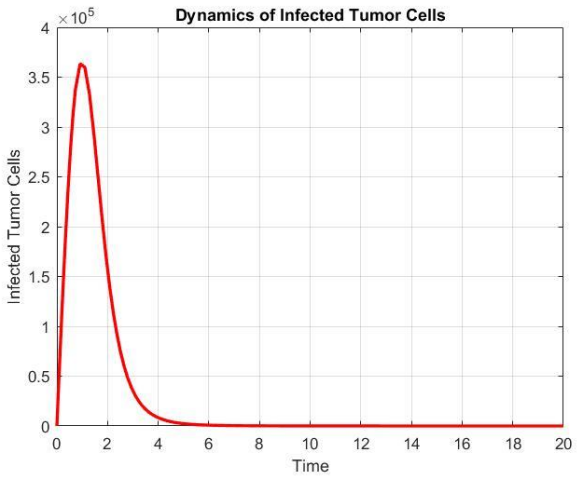

Figure 3: Time evolution of infected tumor cells $I(t)$ under baseline parameter values.

Figure 3, illustrates the infected cell population. Initially, I increases sharply as viral replication dominates. Over time, immune Cells (T) and viral clearance (δ_V) reduce the infected population. If the immune response is strong, I declines toward elimination; otherwise, it persists, indicating a chronic infection state.

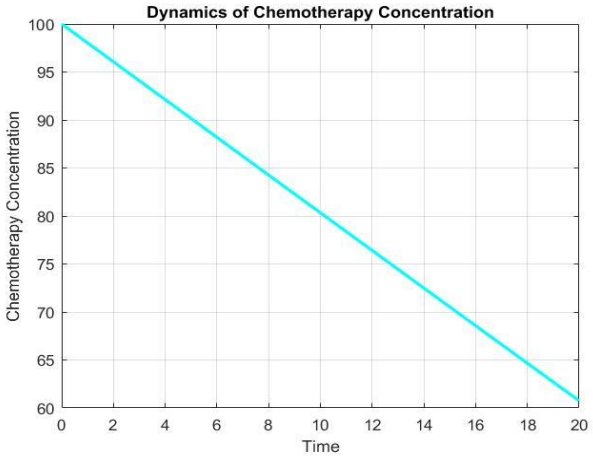

Figure 4: Effect of the control factor $I(t)$ on system stability.

Figure 4, highlights the role of the control factor C, which introduces a regulatory feedback through its saturation kinetics (h_1, h_2). When g is large, C accumulates and suppresses excessive cell growth and infection spread. However, under low g or strong saturation effects, C is insufficient to stabilize the system, allowing infection to persist. This finding underlines the potential role of control mechanisms in therapeutic interventions.

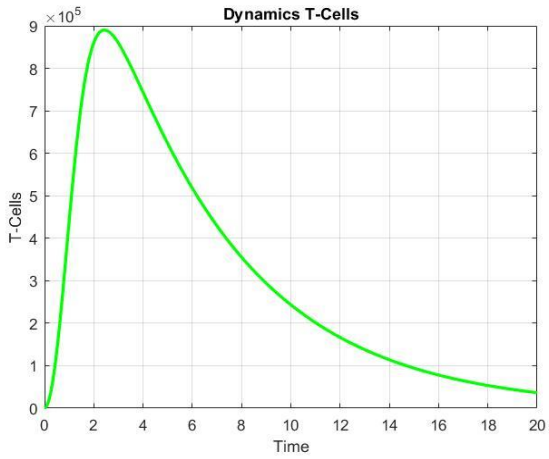

Figure 5: Dynamics of effector cells $E(t)$ and their impact on infection control.

Figure 4, the T-cells population increases in response to the presence of infected cells. A higher T-cells production rate (ϕ_I) enhances infection clearance, reflected by reduced viral and infected cell levels. Conversely, when T-cells decay (δ_T) dominates, the immune response becomes insufficient, leading to persistent infection. These results emphasize the importance of sustained T-cells activity in longterm infection control.

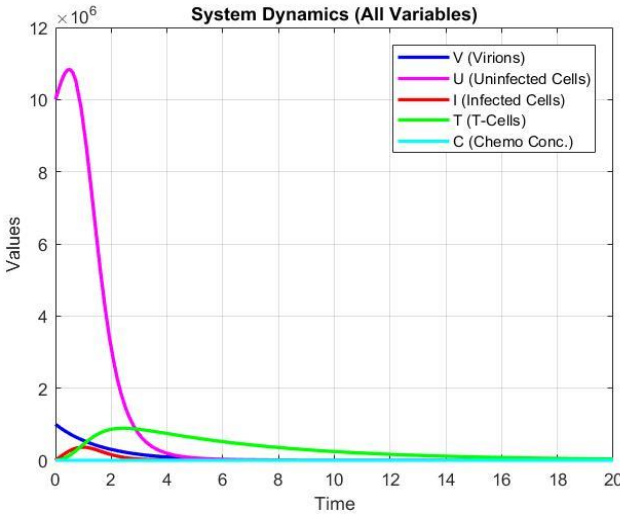

Figure 6: Time evolution of viral particles $V(t)$, uninfected cells $U(t)$ infected cells $I(t)$, Chemotherapy $C(t)$, and immune Cells $t(t)$ under baseline parameter values.

Figure 6, illustrates the complete system dynamics. The viral population $V(t)$ initially expands, driving an increase in infected cells $I(t)$ while simultaneously depleting uninfected cells $U(t)$. As infection progresses, immune-mediated effects and viral clearance reduce both V and I, permitting partial recovery of U.

The chemotherapy $C(t)$ rises early but stabilizes due to its saturation term, representing limited regulatory capacity. T-cells $T(t)$ increase in response to infection, peak during the active viral phase, and then level off as natural decay balances stimulation.

Taken together, the trajectories demonstrate the interplay between viral replication, immune surveillance, and regulatory feedback. The model captures how infection can initially overwhelm the system, yet immune responses and control mechanisms act to restore balance over time.

DISCUSSION

The analysis confirms that the system is biologically well defined: every variable remains nonnegative and bounded, reflecting realistic biological constraints. Numerical simulations further illustrate how different mechanisms contribute to infection control. For instance, the parameter δ_V, representing viral clearance, directly limits the persistence of viral particles; when its value increases, the viral population declines more rapidly, preventing uncontrolled growth. Similarly, the T-cells related parameters γ_U and γ_I capture the immune system's ability to eliminate infected and uninfected cells, respectively. Simulations show that stronger immune responses (larger γ_U or γ_I) suppress infection more efficiently, which aligns with experimental observations in immunology.

The logistic growth parameter r and the carrying capacity K regulate the population of uninfected cells. In the absence of infection, $U(t)$ stabilizes near K, but under viral pressure the balance shifts, and survival depends on how rapidly cells are replenished compared to infection and immune destruction. The chemotherapy C, governed by the supply rate g and the saturation constants h_1 and h_2, plays a stabilizing role: it prevents indefinite expansion of cell populations by introducing regulatory feedback. The simulations reveal that saturation effects in C are particularly important, as they can determine whether infection remains under control or escapes regulation.

Taken together, these results emphasize that viral persistence is not merely a consequence of viral replication (α, β) but results from a delicate interplay between replication, immune clearance, and regulatory mechanisms. The model thus provides a framework for testing how changes in parameter values, whether due to natural variability or therapeutic interventions, affect long-term infection dynamics.

CONCUSLION

The proposed model combines rigorous analysis with numerical exploration to capture the essential features of virus–cell–immune interactions. The positivity and boundedness analysis guarantees that the system remains biologically meaningful, while simulations provide a more detailed picture of how key parameters influence outcomes. Strong immune responses and chemotherapy regulatory factors emerge as decisive in controlling viral spread, whereas weak responses or saturation effects may lead to persistence or chronic infection.

This work contributes to the growing body of research demonstrating how mathematical models can illuminate complex biological processes. While the present study captures

the main dynamical features, future extensions are necessary. Incorporating time delays could better describe the lag between infection and immune activation, while spatial extensions might reveal heterogeneity in viral spread within tissues. Parameter estimation using clinical data would increase predictive value and support model-based therapeutic design. Finally, coupling the system with optimal control strategies may help identify effective treatment protocols.

Overall, the study shows that mathematical modeling, supported by both analysis and simulation, is a valuable tool for exploring infection dynamics and guiding biomedical research.

REFERENCES

[1]. Jenner, A. L. (2020). Applications of mathematical modelling in oncolytic virotherapy and immunotherapy. Bulletin of the Australian Mathematical Society, 101(3), 522-524.

[2]. Jenner, A. L., Yun, C. O., Kim, P. S., & Coster, A. C. (2018). Mathematical modelling of the interaction between cancer cells and an oncolytic virus: insights into the effects of treatment protocols. Bulletin of mathematical biology, 80(6), 1615-1629.

[3]. Jenner, A. L., Coster, A. C., Kim, P. S., & Frascoli, F. (2018). Treating cancerous cells with viruses: insights from a minimal model for oncolytic virotherapy.

[4]. Jenner, A. L., Kim, P. S., & Frascoli, F. (2019). Oncolytic virotherapy for tumours following a Gompertz growth law. Journal of theoretical biology, 480, 129-140.

[5]. Jenner, A. L., Frascoli, F., Coster, A. C., & Kim, P. S. (2020). Enhancing oncolytic virotherapy: Observations from a Voronoi Cell-Based model. Journal of Theoretical Biology, 485, 110052.

[6]. Jenner, A. L., Yun, C. O., Yoon, A., Coster, A. C., & Kim, P. S. (2018). Modelling combined virotherapy and immunotherapy: strengthening the antitumour immune response mediated by IL-12 and GM-CSF expression. Letters in Biomathematics, 5(sup1), S99-S116.

[7]. Yadav, M., & Singh, P. (2025). Stability analysis and numerical simulations for interactions of tumor-immune system with drug delivery. Chaos, Solitons & Fractals, 192, 115971.

[8]. Kim, P. S., Crivelli, J. J., Choi, I. K., Yun, C. O., & Wares, J. R. (2015). Quantitative impact of immunomodulation versus oncolysis with cytokine-expressing virus therapeutics. Mathematical biosciences and engineering, 12(4), 841-858.

[9]. Norton, L. (1988). A Gompertzian model of human breast cancer growth. Cancer research, 48(24_Part_1), 7067-7071.

[10]. Diebner, H. H., Zerjatke, T., Griehl, M., & Roeder, I. (2018). Metabolism is the tie: The Bertalanffy-type cancer growth model as common denominator of various modelling approaches. Biosystems, 167, 1-23.

[11]. Murphy, H., Jaafari, H., & Dobrovolny, H. M. (2016). Differences in predictions of ODE models of tumor growth: a cautionary example. BMC cancer, 16(1), 163.

[12]. L. G. de Pillis and A. Radunskaya, "A mathematical model of immune response to tumor invasion," in Computational fluid and solid mechanics 2003, Elsevier, 2003, pp. 1661–1668

[13]. P. Unni and P. Seshaiyer, "Mathematical modeling, analysis, and simulation of tumor dynamics with drug interventions," Comput. Math. Methods Med., vol. 2019, no. 1, p. 4079298, 2019.

[14]. S. Vieira and R. Hoffmann, "Comparison of the logistic and the Gompertz growth functions considering additive and multiplicative error terms," J. R. Stat. Soc. Ser. C Appl. Stat., vol. 26, no. 2, pp. 143–148, 1977.

[15]. L. G. de Pillis, W. Gu, and A. E. Radunskaya, "Mixed immunotherapy and chemotherapy of tumors: modeling, applications and biological interpretations," J. Theor. Biol., vol. 238, no. 4, pp. 841–862, 2006.

Siraj Ahmad MPhil Mhematics, University of Engineering and Technology Peshawar, Pakistan, E-mail: sirajkhan5278@gmail.com

Zia Ullah Afridi MPhil Mathematics, University of Engineering and Technology Peshawar, Pakistan E-mail: ziaafridi932@gmail.com

BiBi Shabana MPhil Mathematics, University of Engineering and Technology Peshawar, Pakistan, E-mail: shabanasamad.27@gmail.com

How to cite this article:

Siraj Ahmad, Zia Ullah Afridi, Bibi Shabana "Modeling and Analysis of Tumor Growth under Virotherapy, Chemotherapy, and Immune System Dynamics" International Journal of Engineering Works, Vol. 12, Issue 10, PP. 191-196, October 2025. https://doi.org/10.5281/zenodo.17360342.